Set-membership vs. stochastic approaches for target localization with UAVs

J. Ibenthal, Michel Kieffer, Hélène Piet-Lahanier, Luc Meyer

Available online at www.sciencedirect.com

ScienceDirect

IFAC Papers Online CONFERENCE PAPER ARCHIVE

IFAC PapersOnLine 56-2 (2023) 3326–3333

Set-membership vs. stochastic approaches for target localization with UAVs

J. Ibenthal [*,**] **M. Kieffer** [**] **H. Piet-Lahanier** [*] **L. Meyer** [*]

[*] *ONERA, DTIS, Univ Paris Saclay, F-91120 Palaiseau, (e-mail: author@onera.fr).*

[**] *Université Paris Saclay - CentraleSupelec - CNRS, L2S, F-91192 Gif-sur-Yvette (e-mail: author@universite-paris-saclay.fr)*

Abstract: Searching and tracking mobile targets rely most often on modeling the uncertainty and various perturbations by stochastic processes. The detection and location of the targets are performed with Bayesian estimation, which reliability and resulting performance are deeply linked to the adequacy of the stochastic models. An alternative approach limits the representation of these perturbations by defining the bounds within which they can vary. Set-membership estimation techniques have been developed to handle this representation. This paper compares the performance of set-membership and stochastic Bayesian estimation techniques for target search and tracking for scenarios integrating false alarms. For this purpose, estimation schemes are presented for each approach. The ability of estimators to find real targets and not to be deceived by false targets or imperfect sensors are compared in simulations.

Keywords: Search and track, mobile targets, UAVs, set-membership estimation, Bayesian estimation, performance comparison.

1. INTRODUCTION

Searching and tracking mobile targets using fleets of UAVs is a challenging problem that encompasses many considerations, such as the confidence for the target presence, the accuracy of the estimated location, the optimal placement of the sensors, the energy consumption, the available search time, and the environmental hazards, see, *e.g.*, Robin and Lacroix (2016) for a survey.

One of the main issues concerns how to model the uncertainties, perturbations in the measurements, and the variability of the quality of detection. This is most often performed by considering that the uncertainties or perturbations are additive noises, which are usually described by Gaussian processes. Moreover, the false alarms or non-detection of targets are assumed to correspond to the realization of random events. The search and track procedures associated to these representations often consider a grid-based probability map of the search zone representing the confidence for potential target locations (Hespanha et al., 1999; Vidal et al., 2001; Bertuccelli and How, 2006b; Furukawa et al., 2006; Yang et al., 2007; Khan et al., 2015). The probability of the presence of a target in each cell can be either modeled as a single value (Yang et al., 2007) or as a stochastic variable with a probability density distribution (pdf) (Bertuccelli and How, 2005, 2006a). The evolution and update of the map are performed by recursive Bayesian filtering. The correction step after measurement accounts for probabilities of true positive and false positive detection but does not explicitly integrate measurement uncertainties (Hu et al., 2012, 2017). Nevertheless, *a priori* pdfs describing the process and measurement noises may not always be available. As pointed out in Gu et al. (2015), the resulting performance may prove sensitive to these *a priori* assumptions.

Alternatively, instead of considering some pdf characterizing the noise distribution, it may be assumed that noise and uncertainties remain within *a priori* known bounds. Then set-membership (SM) estimation techniques can be used to evaluate target state *set estimates*. These techniques are well suited to characterize areas where targets are guaranteed to be present or absent with either deterministic boundaries, as in Drevelle et al. (2013); Desrochers and Jaulin (2016), or with uncertain boundaries, as in Boukezzoula et al. (2021). In Ibenthal et al. (2020, 2021), the widely-used probability of false alarm is replaced by deterministic geometric conditions depending on the target observation point of view. The approach proved to be very robust to the presence of decoys.

This paper compares the performance of SM and stochastic Bayesian estimation techniques for target search and tracking in scenarios integrating false alarms due to decoys or imperfect sensors. The assumptions and modeling of uncertainties and false alarms differ significantly between Bayesian and set membership estimations which makes a straightforward comparison using the approaches presented in the literature really difficult and potentially biased. Therefore, an adapted estimation scheme is presented for each technique considering similar assumptions on the measurement noise and false alarms. The performance of the estimators is compared in simulations considering their ability to find real targets and not to be deceived by false targets or imperfect sensors.

2. PROBLEM FORMULATION

Consider N^{u} identical UAVs searching for an unknown but constant number N^{t} of ground targets evolving in a delimited Region of Interest (RoI) $\mathbb{X}_0 \subset \mathbb{R}^3$, free of any

10.1016/j.ifacol.2023.10.1477

obstacle. All $\mathbf{x} \in \mathbb{X}_0$ are such that $x_3 = 0$. Time is sampled with a constant period T. At time $t_k = kT$, let $\mathbf{x}^{\mathrm{u}}_{i,k} \in \mathbb{R}^{n^{\mathrm{u}}}$ be the state vector of UAV $i \in \mathcal{N}^{\mathrm{u}} = \{1, \dots, N^{\mathrm{u}}\}$ and $\mathbf{x}^{\mathrm{t}}_{j,k} \in \mathbb{X}_0$ is the state vector of target $j \in \mathcal{N}^{\mathrm{t}} = \{1, \dots, N^{\mathrm{t}}\}$.

The evolution with time of the UAV state is modeled as

$$\mathbf{x}^{\mathrm{u}}_{i,k+1} = \mathbf{f}^{\mathrm{u}}_k \left(\mathbf{x}^{\mathrm{u}}_{i,k}, \mathbf{u}_{i,k}\right), \tag{1}$$

where $\mathbf{f}^{\mathrm{u}}_k$ is known function. The control input $\mathbf{u}_{i,k}$ of UAV i is constrained in a set $\mathbb{U}$ of admissible control inputs. The state $\boldsymbol{x}^{\mathrm{t}}_{j,k}$ of target j evolves as

$$\mathbf{x}^{\mathrm{t}}_{j,k+1} = \mathbf{x}^{\mathrm{t}}_{j,k} + T\mathbf{v}_{j,k}, \tag{2}$$

where $\mathbf{v}_{j,k}$ is its velocity assumed piecewise constant over the time intervals $[t_k, t_{k+1}[$. The target heading angle $\gamma(\mathbf{v}_{j,k})$ is only known to belong to $[0, 2\pi[$, and the magnitude $\|\mathbf{v}_{j,k}\|$ of its velocity is assumed bounded in $[0, v]$.

The sensor of each UAV i has a limited field-of-view (FoV), *i.e.*, UAV i is only able to observe a subset $\mathbb{F}_i(\mathbf{x}^{\mathrm{u}}_{i,k})$ of the space, *e.g.*, a half-cone. At time $t_k = kT$, after processing the information in the FoV $\mathbb{F}_i(\mathbf{x}^{\mathrm{u}}_{i,k})$, UAV i obtains a list of measurements $\mathcal{Y}_{i,k} = \{\mathbf{y}_{i,m,k}\}_{m \in \mathcal{D}_{i,k}}$ related to the targets present in the FoV, *i.e.*,

$$\boldsymbol{x}^{\mathrm{t}}_{j,k} \in \mathbb{F}_i\left(\mathbf{x}^{\mathrm{u}}_{i,k}\right) \Rightarrow \exists \mathbf{y} \in \mathcal{Y}_{i,k} \text{ such that } \mathbf{y} = \mathbf{y}_{i,j,k}. \tag{3}$$

Targets present in the FoV are thus always detected. Nevertheless, we assume that UAVs are unaware of the list of indexes $\mathcal{D}_{i,k} \subset \mathcal{N}^{\mathrm{u}}$ of the detected targets, *i.e.*, a measurement cannot be associated to a specific target. For each $m \in \mathcal{D}_{i,k}$, the measurement vector is

$$\mathbf{y}_{i,m,k} = \mathbf{h}_i\left(\mathbf{x}^{\mathrm{u}}_{i,k}, \mathbf{x}^{\mathrm{t}}_{j,k}\right) + \mathbf{w}_{i,m,k}, \tag{4}$$

where $\mathbf{h}_i$ is the measurement equation of UAV i and $\mathbf{w}_{i,m,k}$ is the measurement noise, assumed bounded in some box $[\mathbf{w}_{i,m,k}]$. Usually the size of $[\mathbf{w}_{i,m,k}]$ depends on the environmental and measurement conditions Cortes et al. (2004); Li and Duan (2017). One assumes that a known box $[\mathbf{w}]$ such that $[\mathbf{w}_{i,m,k}] \subset [\mathbf{w}]$ is available considering, *e.g.*, worst-case measurement conditions.

False positive detection may occur due to decoys or lures confused with targets, changing environmental conditions (such as natural lighting), or imperfections of the measurement processing system. As a consequence, the list $\mathcal{Y}_{i,k}$ may contain measurements that do not correspond to a true target. At this point, no specific model for false positive detection is assumed. False positive detection may be deterministic or probabilistic.

In what follows, two approaches for target search and tracking are presented. Both approaches are able to account for potential false positive detection of targets in their estimation scheme. The bounds for $\gamma(\mathbf{v}_{j,k})$ and $\|\mathbf{v}_{j,k}\|$ and the measurement noise bounds $[\mathbf{w}]$ are available for both approaches.

3. SET-MEMBERSHIP ESTIMATION

This section describes a simplified version of the SM estimator presented in Ibenthal et al. (2021). At time t_k, UAV i maintains three sets: $\mathbb{X}_{i,k} \subset \mathbb{X}_0$ contains all possible target state values consistent with the information $\mathcal{I}_{i,k}$ available to UAV i up to time t_k, $\overline{\mathbb{X}}_{i,k} \subset \mathbb{X}_0$ contains the possible state values of targets not yet detected, and $\widetilde{\mathbb{X}}_{i,k} = \mathbb{X}_0 \setminus \left(\mathbb{X}_{i,k} \cup \overline{\mathbb{X}}_{i,k}\right)$ is the explored subset of $\mathbb{X}_0$ and is known not to contain any true target state. Due to potential false positive detection, $\mathbb{X}_{i,k}$ may contain state values not consistent with actual target states.

The relative estimation uncertainty for UAV i in the SM context is

$$\Phi^{\mathrm{SM}}\left(\mathbb{X}_{i,k}, \overline{\mathbb{X}}_{i,k}\right) = \phi\left(\mathbb{X}_{i,k} \cup \overline{\mathbb{X}}_{i,k}\right) / \phi\left(\mathbb{X}_0\right), \tag{5}$$

where ϕ is some measure function, *e.g.*, the area or volume of the sets. The aim of each UAV i is to reduce $\Phi^{\mathrm{SM}}\left(\mathbb{X}_{i,k}, \overline{\mathbb{X}}_{i,k}\right)$ as much as possible.

3.1 Evolution of the set estimates

At time t_k, UAV i has access to $\mathbb{X}_{i,k}$ and $\overline{\mathbb{X}}_{i,k}$. These sets are updated to $\mathbb{X}_{i,k+1}$ and $\overline{\mathbb{X}}_{i,k+1}$ at time t_{k+1} using the target evolution model (2), the list $\mathcal{Y}_{i,k+1}$ of collected measurements, and the information received from neighbors in $\mathcal{N}_{i,k+1} \subset \mathcal{N}^{\mathrm{u}}$ with which UAV i is able to communicate. At time t_0, for UAV i, one has $\mathbb{X}_{i,0} = \emptyset$ and $\overline{\mathbb{X}}_{i,0} = \mathbb{X}_0$.

The estimator starts with a *prediction step*. At time t_k, from (2), UAV i evaluates the set of predicted target locations

$$\begin{aligned}\mathbb{X}_{i,k+1|k} = \big\{\mathbf{x} + T\mathbf{v} \,|\, \mathbf{x} \in \mathbb{X}_{i,k}, \mathbf{v} \in \mathbb{R}^2,\\ \|\mathbf{v}\| < v, \gamma(\mathbf{v}_{j,k}) \in [0, 2\pi[\} \cap \mathbb{X}_0,\end{aligned} \tag{6}$$

that can be reached from any $\mathbf{x} \in \mathbb{X}_{i,k}$ at time t_{k+1}. The set $\overline{\mathbb{X}}_{i,k+1|k}$ is evaluated similarly from $\overline{\mathbb{X}}_{i,k}$.

At time t_{k+1}, a *correction step from measurements* is performed exploiting the list of measurements $\mathcal{Y}_{i,k+1}$ obtained form the observed FoV $\mathbb{F}_i(\mathbf{x}^{\mathrm{u}}_{i,k+1})$. From $\mathcal{Y}_{i,k+1}$, the measurement model (4), and the bounds $[\mathbf{w}]$ on the measurement noise, the set containing all noise-free measurements is

$$\mathbb{Y}_{i,k} = \{\mathbf{y} - \mathbf{w} \,|\, \mathbf{y} \in \mathcal{Y}_{i,k}, \mathbf{w} \in [\mathbf{w}]\}. \tag{7}$$

Then, different cases have to be considered to determine the set $\mathbb{X}_{i,k+1|k+1}$ updated from $\mathbb{X}_{i,k+1|k}$. Target detected at time t_{k+1} may correspond to already detected targets which state is inside $\mathbb{X}_{i,k+1|k}$. From (4), the associated set estimate is

$$\mathbb{S}_1 = \left\{\mathbf{x} \in \mathbb{X}_{i,k+1|k} \,|\, \mathbf{h}_{k+1}(\mathbf{x}^{\mathrm{u}}_{i,k+1}, \mathbf{x}) \in \mathbb{Y}_{i,k}\right\}. \tag{8}$$

Alternatively, targets may be detected for the first time in $\overline{\mathbb{X}}_{i,k+1|k}$ and the corresponding set of possible target state values is

$$\mathbb{S}_2 = \left\{\mathbf{x} \in \overline{\mathbb{X}}_{i,k+1|k} \,|\, \mathbf{h}_{k+1}(\mathbf{x}^{\mathrm{u}}_{i,k+1}, \mathbf{x}) \in \mathbb{Y}_{i,k}\right\}. \tag{9}$$

Since target non-detection does not occur, when all information in $\mathbb{F}_i(\mathbf{x}^{\mathrm{u}}_{i,k})$ is processed, there is no target in $\mathbb{F}_i(\mathbf{x}^{\mathrm{u}}_{i,k+1}) \setminus (\mathbb{S}_1 \cup \mathbb{S}_2)$. The set

$$\mathbb{S}_3 = \mathbb{X}_{i,k+1|k} \setminus \mathbb{F}_i\left(\mathbf{x}^{\mathrm{u}}_{i,k+1}\right), \tag{10}$$

contains the target states in the part of $\mathbb{X}_{i,k+1|k}$ outside of the FoV of the UAV i. The updated set estimate $\mathbb{X}_{i,k+1|k+1}$ accounting the three previous cases is then

$$\mathbb{X}_{i,k+1|k+1} = \mathbb{S}_1 \cup \mathbb{S}_2 \cup \mathbb{S}_3. \tag{11}$$

When all measurements from $\mathbb{F}_i(\mathbf{x}^{\mathrm{u}}_{i,k+1})$ are processed, the set $\overline{\mathbb{X}}_{i,k+1|k}$ can be updated as

$$\overline{\mathbb{X}}_{i,k+1|k+1} = \overline{\mathbb{X}}_{i,k+1|k} \setminus \mathbb{F}_i(\mathbf{x}^{\mathrm{u}}_{i,k+1}). \tag{12}$$

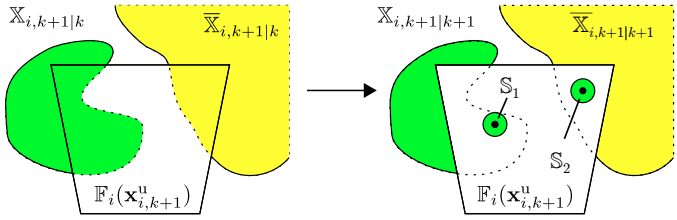

Fig. 1. Set estimates $\mathbb{X}_{i,k+1|k}$ (in green) and $\overline{\mathbb{X}}_{i,k+1|k}$ (in yellow) before correction from measurement (left) and set estimates $\mathbb{X}_{i,k+1|k+1}$ (in green) and $\overline{\mathbb{X}}_{i,k+1|k+1}$ (in yellow) after correction (right).

Figure 1 illustrates a situation where both $\mathbb{S}_1$ and $\mathbb{S}_2$ are not empty, and shows the reduction of the sizes of $\mathbb{X}_{i,k+1|k+1}$ and $\overline{\mathbb{X}}_{i,k+1|k+1}$ compared to those of $\mathbb{X}_{i,k+1|k}$ and $\overline{\mathbb{X}}_{i,k+1|k}$ due to the parts of the FoV $\mathbb{F}_i(\mathbf{x}^{\mathrm{u}}_{i,k+1})$ in which no target is detected.

Finally, once the correction step from measurements is completed, UAV i exchanges the set estimates $\mathbb{X}_{i,k+1|k+1}$ and $\overline{\mathbb{X}}_{i,k+1|k+1}$ with its neighboring UAVs with index $\ell \in \mathcal{N}_{i,k}$, and receives the corresponding sets $\mathbb{X}_{\ell,k+1|k+1}$ and $\overline{\mathbb{X}}_{\ell,k+1|k+1}$. After communication, the set estimate $\mathbb{X}_{i,k+1}$ is evaluated as the union of the set estimates $\mathbb{X}_{\ell,k+1|k+1}$, $\ell \in \mathcal{N}_{i,k+1} \cup \{i\}$ reduced by the union of subsets $\widetilde{\mathbb{X}}_{\ell,k+1|k+1} = \mathbb{X}_0 \setminus \left(\mathbb{X}_{i,k+1|k+1} \cup \overline{\mathbb{X}}_{i,k+1|k+1}\right)$ of $\mathbb{X}_0$ proved not to contain any target state, *i.e.*,

$$\mathbb{X}_{i,k+1} = \bigcup_{\ell \in \mathcal{N}_{i,k+1} \cup \{i\}} \mathbb{X}_{\ell,k+1|k+1} \setminus \bigcup_{\ell \in \mathcal{N}_{i,k+1} \cup \{i\}} \widetilde{\mathbb{X}}_{\ell,k+1|k+1}. \quad (13)$$

Finally, the set estimate $\overline{\mathbb{X}}_{i,k+1}$ is the intersection of the unexplored space of UAV i and that of its neighbors, *i.e.*,

$$\overline{\mathbb{X}}_{i,k+1} = \bigcap_{\ell \in \mathcal{N}_{i,k+1} \cup \{i\}} \overline{\mathbb{X}}_{\ell,k+1|k+1}. \quad (14)$$

Figure 2 illustrates the sets resulting from (13) and (14) for two cases. The size of $\mathbb{X}_{i,k+1}$ may be smaller than $\mathbb{X}_{i,k+1|k+1}$ as in Figure 2 a), when some subsets of $\mathbb{X}_{i,k+1|k+1}$ have been proved by another UAV not to contain a target. It may also be larger, as in Figure 2 b), where UAV ℓ has obtained measurements leading to another hypothesis on the state estimate of a target. The size of $\overline{\mathbb{X}}_{i,k+1}$ is always reduced compared to that of $\overline{\mathbb{X}}_{i,k+1|k+1}$.

3.2 Cooperative control design

At each time t_k, UAV i determines the sequence of control inputs $\mathbf{u}_{i,k:k+h-1} = (\mathbf{u}_{i,k}, \ldots, \mathbf{u}_{i,k+h-1})$ which minimizes the predicted estimation uncertainty $\Phi^{\mathrm{SM}}(\mathbb{X}_{i,k+h}, \overline{\mathbb{X}}_{i,k+h})$ at time t_{k+h}, where $h \geqslant 1$ is the prediction horizon. A model predictive control approach is considered.

At time t_k, UAV i has access to $\mathbb{X}_{i,k}$ and $\overline{\mathbb{X}}_{i,k}$. Using a prediction step described in Section 3.1, UAV i can evaluate $\mathbb{X}_{i,k+1|k}$ and $\overline{\mathbb{X}}_{i,k+1|k}$. Then, for a given control input $\mathbf{u}_{i,k}$, UAV i is able to get a predicted value $\mathbf{x}^{\mathrm{u,p}}_{i,k+1}$ of its state $\mathbf{x}^{\mathrm{u}}_{i,k+1}$ at time t_{k+1} and to infer the corresponding FoV $\mathbb{F}_i(\mathbf{x}^{\mathrm{u,p}}_{i,k+1})$. Nevertheless, UAV i is unable to determine whether it will observe new or previously detected targets in $\mathbb{F}_i(\mathbf{x}^{\mathrm{u,p}}_{i,k+1})$. Consequently, neglecting also the

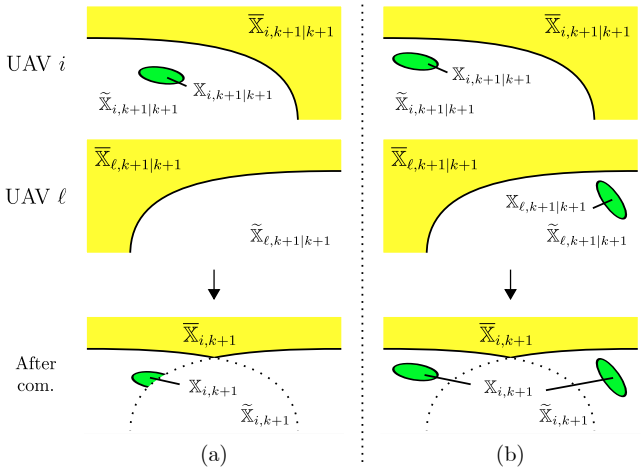

Fig. 2. Set estimates evaluated by UAV i and ℓ before communication (two top subfigures of each column) and after communication and update (bottom subfigures).

information provided by other UAVs, in the correction from measurement step described in Section 3.1, only the impact of the reduction of the sets due to the FoV is evaluated to get the predicted values

$$\mathbb{X}^{\mathrm{p}}_{i,k+1} = \mathbb{X}_{i,k+1|k} \setminus \mathbb{F}_i(\mathbf{x}^{\mathrm{u,p}}_{i,k+1}), \quad (15)$$

$$\overline{\mathbb{X}}^{\mathrm{p}}_{i,k+1} = \overline{\mathbb{X}}_{i,k+1|k} \setminus \mathbb{F}_i(\mathbf{x}^{\mathrm{u,p}}_{i,k+1}). \quad (16)$$

A predicted estimation uncertainty for UAV i at time t_{k+1} may be evaluated as $\Phi^{\mathrm{SM}}(\mathbb{X}^{\mathrm{p}}_{i,k+1}, \overline{\mathbb{X}}^{\mathrm{p}}_{i,k+1})$ and is a lower bound of the uncertainty that can be achieved.

The previous approach may be applied iteratively on $\mathbb{X}^{\mathrm{p}}_{i,k+\kappa}$ and $\overline{\mathbb{X}}^{\mathrm{p}}_{i,k+\kappa}$ to evaluate the impact of $\mathbf{u}_{i,k+\kappa}$, $\kappa = 1, \ldots, h-1$, on the predicted estimation uncertainty for UAV i at time $t_{k+\kappa}$, which provides $\mathbb{X}^{\mathrm{p}}_{i,k+h}$ and $\overline{\mathbb{X}}^{\mathrm{p}}_{i,k+h}$ when $\kappa = h-1$. Thus an estimate $\Phi^{\mathrm{SM}}(\mathbb{X}^{\mathrm{p}}_{i,k+h}, \overline{\mathbb{X}}^{\mathrm{p}}_{i,k+h})$ of $\Phi^{\mathrm{SM}}(\mathbb{X}_{i,k+h}, \overline{\mathbb{X}}_{i,k+h})$ is deduced. In practice, UAV i searches the sequence of control inputs $\mathbf{u}_{i,k:k+h-1}$ minimizing

$$J\left(\mathbf{u}_{i,k:k+h-1}\right) = \Phi^{\mathrm{SM}}(\mathbb{X}^{\mathrm{p}}_{i,k+h}, \overline{\mathbb{X}}^{\mathrm{p}}_{i,k+h}) + \alpha^{\mathrm{SM}} d_{\mathrm{H}}(\mathbf{x}^{\mathrm{u,p}}_{i,k+h}, \mathbb{X}^{\mathrm{p}}_{i,k+h} \cup \overline{\mathbb{X}}^{\mathrm{p}}_{i,k+h}), \quad (17)$$

where $d_{\mathrm{H}}(\mathbf{x}, \mathbb{X})$ is the Hausdorff distance between the vector $\mathbf{x}$ and the set $\mathbb{X}$. The second term is introduced to drive UAV i towards $\mathbb{X}^{\mathrm{p}}_{i,k+h}$ or $\overline{\mathbb{X}}^{\mathrm{p}}_{i,k+h}$ when the first term, $\Phi^{\mathrm{SM}}(\mathbb{X}^{\mathrm{p}}_{i,k+h}, \overline{\mathbb{X}}^{\mathrm{p}}_{i,k+h})$, remains constant, whatever the sequence of inputs $\mathbf{u}_{i,k:k+h-1}$, which may occur when the chosen prediction horizon is not large enough. The parameter α^{SM} adjusts the relative importance of the second term.

A cooperative version of the previous control strategy is considered where UAVs evaluate their control input sequentially. For example, UAV i accounts for the predicted sets $\mathbb{X}^{\mathrm{p}}_{\ell,k+h}$ and $\overline{\mathbb{X}}^{\mathrm{p}}_{\ell,k+h}$ of neighbors with index $\ell \in \mathcal{N}^{\mathrm{c}}_{i,k} \subseteq \mathcal{N}_{i,k}$, which have already evaluated their sequence of control inputs. These sets may be used for the control design of neighboring UAVs in the prediction approach to account for predicted estimates of other UAVs using (13) and (14), see Ibenthal et al. (2021) for more details.

4. BAYESIAN ESTIMATION FOR TARGET SEARCH AND TRACK IN A STOCHASTIC CONTEXT

This section presents an adaptation of the Bayesian state estimation approach in a stochastic context for target search and tracking of Hu et al. (2012, 2014). The approach evaluates the *a posteriori* probability of presence of a target in a discrete probability grid of the RoI. The approach is adapted to account for the partly unknown target dynamics and to comply with the observation model introduced in (4). Here, we assume that $\gamma(\mathbf{v}_{j,k})$ and $\|\mathbf{v}_{j,k}\|$ are uniformly distributed in $[0, 2\pi[$ and $[0, v]$ respectively and that $\mathbf{w}_{i,j,k}$ is uniformly distributed in $[\mathbf{w}]$.

Following the approach in Hu et al. (2014), $\mathbb{X}_0$ is partitioned into N^{c} regular rectangular cells $\mathcal{C}_m \subset \mathbb{X}_0$, where $m \in \mathcal{N}^{\mathrm{c}} = \{1, \ldots, N^{\mathrm{c}}\}$. Assume that there is at most one target in each cell. At time t_k, let θ_k^m be a Bernoulli random variable indicating the presence ($\theta_k^m = 1$) or absence ($\theta_k^m = 0$) of a target in cell $\mathcal{C}_m$. The aim of UAV i is to evaluate $p_{i,k}^m = \Pr(\theta_k^m = 1 \mid \mathcal{I}_{i,k})$, the posterior probability of presence of a target in $\mathcal{C}_m$ considering all information $\mathcal{I}_{i,k}$ available to UAV i up to time t_k. The *probability map* $\mathcal{P}_{i,k} = \{p_{i,k}^m\}_{m \in \mathcal{N}^{\mathrm{c}}}$ gathers all values of $p_{i,k}^m$ at time t_k.

In the Bayesian approach, two ingredients are instrumental. The first is the transition probability $\Pr(\theta_{n,k+1} = 1 \mid \theta_{m,k} = 1)$ providing the probability that a target is in cell n at time t_{k+1} knowing that there is a target in cell m at time t_k. The transition probability is assumed to be time invariant and can be evaluated assuming a single target present in the RoI in cell m. The pdf $p_k(\mathbf{x})$ of the target state can be assumed uniform over $\mathcal{C}_m$ and null outside of $\mathcal{C}_m$. Then, a continuous target state transition pdf $\pi(\mathbf{x}'|\mathbf{x})$ to represent the displacement of a target during a time interval of duration T may be derived from the target dynamics (2), as described, *e.g.*, in Zhen et al. (2020). The pdf of the predicted target location $p_{k+1|k}(\mathbf{x})$ at time t_{k+1} is obtained via the Chapman-Kolmogorov equation as

$$p_{k+1|k}(\mathbf{x}) = \int_{\mathbb{X}_0} \pi(\mathbf{x}' \mid \mathbf{x})\, p_k(\mathbf{x})\, \mathrm{d}\mathbf{x}. \tag{18}$$

The transition probability $\Pr(\theta_{n,k+1} = 1 \mid \theta_{m,k} = 1)$ is then obtained integrating $p_{k+1|k}(\mathbf{x})$ over $\mathcal{C}_n$, $n \in \mathcal{N}^{\mathrm{c}}$.

The second is the processing of observations. At time t_{k+1}, UAV i observes $\mathbb{F}_i(\mathbf{x}_{i,k+1}^{\mathrm{u}})$ and gets $\mathbb{Y}_{i,k+1}$. It can evaluate the list of *completely* observed cells

$$\mathcal{O}_{i,k+1} = \left\{ m \in \mathcal{N}^{\mathrm{c}} \mid \mathcal{C}_m \subset \mathbb{F}_i\left(\mathbf{x}_{i,k+1}^{\mathrm{u}}\right) \cap \mathbb{X}_0 \right\}.$$

and a list of cells where targets are detected

$$\mathcal{L}_{i,k+1} = \left\{ m \in \mathcal{N}^{\mathrm{c}} \mid \exists \mathbf{x} \in \mathcal{C}_m, \mathbf{h}_i\left(\mathbf{x}_{i,k+1}^{\mathrm{u}}, \mathbf{x}\right) \in \mathbb{Y}_{i,k} \right\}.$$

From $\mathcal{O}_{i,k+1}$ and $\mathcal{L}_{i,k+1}$, UAV i deduces the *observation result* $z_{i,k+1}^m$ for cell m. If $m \in \mathcal{L}_{i,k+1}$, then $z_{i,k}^m = 1$, indicating that a target is detected in $\mathcal{C}_m$. If $m \in \mathcal{O}_{i,k+1}$ and $m \notin \mathcal{L}_{i,k+1}$, then $z_{i,k}^m = 0$, indicating that not target is detected in the observed cell $\mathcal{C}_m$. One assumes further that the true positive detection probability is $\Pr(z_{i,k}^m = 1|\theta_k^m = 1) = p$ and the false positive detection probability is $\Pr(z_{i,k}^m = 1|\theta_k^m = 0) = q$. Here, one has $p = 1$ since targets located inside the FoV are always detected, see Section 2, and $q > 0$ since it is assumed that false positive detection of targets may appear. Conditioned on θ_k^m, the random variables $z_{i,k}^m$ are assumed to be time-independent.

For a given threshold $\underline{p} \in [0.5, 1]$, the relative estimation uncertainty for UAV i in the Bayesian (B) estimation context is

$$\Phi^{\mathrm{B}}\left(\mathcal{P}_{i,k}, \underline{p}\right) = \left|\{m \in \mathcal{N}^{\mathrm{c}} \mid 1 - \underline{p} < p_{i,k}^m < \underline{p}\}\right| / N^{\mathrm{c}}, \tag{19}$$

where $|\mathcal{N}|$ is the cardinal number of the set $\mathcal{N}$. The function $\Phi^{\mathrm{B}}\left(\mathcal{P}_{i,k}, \underline{p}\right)$ evaluates the proportion of cells with $p_{i,k}^m$ close to 1/2, *i.e.*, the presence or absence of target is still uncertain. The tolerated level of uncertainty is determined by $\underline{p}$.

4.1 Evolution of the probability map

At time t_k, to evaluate $\mathcal{P}_{i,k+1}$ from $\mathcal{P}_{i,k}$, UAV i applies a three-step estimation procedure similar to that in Section 3. At time t_0, the probability of presence of a target in each cell is chosen as $p_{i,k}^m = p_0 = 0.5$, $m \in \mathcal{N}^{\mathrm{c}}$, to represent the fact that targets may be anywhere in the RoI.

First, a *prediction step* is applied to evaluate $p_{i,k+1|k}^n = \Pr\left(\theta_{k+1}^n = 1 \mid \mathcal{I}_{i,k}\right)$, $n \in \mathcal{N}^{\mathrm{c}}$, using

$$p_{i,k+1|k}^n = \sum_{m \in \mathcal{N}^{\mathrm{c}}} \Pr\left(\theta_{k+1}^n = 1 \mid \theta_k^m = 1\right) p_{i,k}^m. \tag{20}$$

This procedure may be compactly written as

$$\mathcal{P}_{i,k+1|k} = M\left(\mathcal{P}_{i,k}\right), \tag{21}$$

where $\mathcal{P}_{i,k+1|k} = \{p_{i,k+1|k}^m\}_{m \in \mathcal{N}^{\mathrm{c}}}$. The function M depends on (20) and can be evaluated offline as the state transition probability does not depend of the target state, see Bertuccelli and How (2006a); Frew and Elston (2008).

At time t_{k+1}, a *correction step from measurements* is performed. Following Khan et al. (2015); Kuhlman et al. (2017), UAV i can evaluate $p_{i,k+1|k+1}^m = \Pr(\theta_{k+1}^m = 1 \mid \mathcal{I}_{i,k}, \mathbb{F}_i(\mathbf{x}_{i,k+1}^{\mathrm{u}}), \mathbb{Y}_{i,k+1})$, $m \in \mathcal{N}^{\mathrm{c}}$ from $\mathcal{P}_{i,k+1|k}$ and $\{z_{i,k+1}^m\}_{m \in \mathcal{N}^{\mathrm{c}}}$ using Bayes' rule. If $m \in \mathcal{O}_{i,k+1}$ and $z_{i,k+1}^m = 1$, one gets

$$p_{i,k+1|k+1}^m = \frac{p.p_{i,k+1|k}^m}{p.p_{i,k+1|k}^m + q(1 - p_{i,k+1|k}^m)}, \tag{22}$$

else if $m \in \mathcal{O}_{i,k+1}$ and $z_{i,k+1}^m = 0$, one has

$$p_{i,k+1|k+1}^m = \frac{(1-p)\, p_{i,k}^m}{(1-p)\, p_{i,k+1|k}^m + (1-q)\left(1 - p_{i,k+1|k}^m\right)}, \tag{23}$$

and if $m \notin \mathcal{O}_{i,k+1}$, one simply gets $p_{i,k+1|k+1}^m = p_{i,k+1|k}^m$. When the detection probability is $p = 1$, $m \in \mathcal{O}_{i,k+1}$ and $z_{i,k+1}^m = 0$ (cell $\mathcal{C}_m$ is in the FoV and no target is detected) leads to $p_{i,k+1|k+1}^m = 0$.

Then, UAV i broadcasts $p_{i,k+1|k+1}^m$ and receives the corresponding information from its neighbors UAV $\ell \in \mathcal{N}_{i,k}$. Then UAV i evaluates $p_{i,k+1}^n = \Pr\left(\theta_{k+1}^n = 1 \mid \mathcal{I}_{i,k+1}\right)$, $n \in \mathcal{N}^{\mathrm{c}}$, using a *correction step from communication,* as in Hu et al. (2012). First the log *a posteriori* ratios

$$q_{i,k+1|k+1}^m = \log\left(\left(1 - p_{i,k+1|k+1}^m\right) / p_{i,k+1|k+1}^m\right), \tag{24}$$

are evaluated and $p_{i,k+1}^m$ is evaluated from

$$q_{i,k+1}^m = \sum_{\ell \in \mathcal{N}_{i,k} \cup \{i\}} w_{i,\ell,k}\, q_{i,k+1|k+1}^m, \tag{25}$$

where $w_{i,i,k} = 1 - ((|\mathcal{N}_{i,k}| - 1)/N^{\mathrm{u}})$ and $w_{i,\ell,k} = 1/N^{\mathrm{u}}$, $\ell \in \mathcal{N}_{i,k}$, applying the inverse of (24) to get finally $\mathcal{P}_{i,k+1}$.

4.2 Control design

As in Section 3.2, each UAV i searches a sequence of control inputs $\mathbf{u}_{i,k:k+h-1}$ which minimizes the uncertainty $\Phi^{\mathrm{B}}(\mathcal{P}_{i,k+h}, \underline{p})$ at time t_{k+h}. To get a fair comparison, a model predictive control approach relying on the same assumptions as in Section 3.2 is considered: (1) UAVs compute their control inputs sequentially, (2) once $\mathbf{u}_{i,k:k+h-1}$ is evaluated, it is broadcast, (3) UAV i accounts for the control sequences of neighbors in $\ell \in \mathcal{N}^{\mathrm{c}}_{i,k} \subseteq \mathcal{N}_{i,k}$, and (4) UAVs are unable to predict whether a target will be detected at $t_{k+\kappa}$, $\kappa = 1 \ldots, h$.

At time t_k, UAV i has access to $\mathcal{P}_{\ell,k}$ and $\mathbf{x}^{\mathrm{u,p}}_{\ell,k+1:k+h}$, $\ell \in \mathcal{N}^{\mathrm{c}}_{i,k}$. For a control input $\mathbf{u}_{i,k}$, UAV i predicts $\mathbf{x}^{\mathrm{u}}_{i,k+1}$ to get $\mathbf{x}^{\mathrm{u,p}}_{i,k+1}$ using (1). The predicted map $\mathcal{P}^{\mathrm{p}}_{\ell,k+1|k}$ is evaluated from $\mathcal{P}_{\ell,k}$ using (21). At t_{k+1},the predicted set of entirely observed cells by UAV i or one of its neighbors is

$$\mathcal{O}^{\mathrm{p}}_{\ell,k+1} = \left\{ m \in \mathcal{N}^{\mathrm{c}} \mid \mathcal{C}_m \subset \mathbb{F}_\ell(\mathbf{x}^{\mathrm{u}}_{\ell,k+1}) \cap \mathbb{X}_0 \right\}, \tag{26}$$

with $\ell \in \mathcal{N}^{\mathrm{c}}_{i,k} \cup \{i\}$. As UAVs are unable to predict whether targets will be detected, the predicted value of $\mathcal{L}_{\ell,k+1}$ is $\mathcal{L}^{\mathrm{p}}_{\ell,k+1} = \emptyset$ and that of $z^m_{\ell,k+1}$ is $z^{m,\mathrm{p}}_{\ell,k+1} = 0$, for $m \in \mathcal{O}^{\mathrm{p}}_{\ell,k+1}$ and $\ell \in \mathcal{N}^{\mathrm{c}}_{i,k} \cup \{i\}$. $\mathcal{P}^{\mathrm{p}}_{\ell,k+1|k+1}$ is then deduced from $\mathcal{P}^{\mathrm{p}}_{\ell,k+1|k}$ and the $z^{m,\mathrm{p}}_{\ell,k+1}$s using (22) and (23). Finally, $\mathcal{P}^{\mathrm{p}}_{i,k+1}$ is obtained from $\mathcal{P}^{\mathrm{p}}_{\ell,k+1|k+1}$, $\ell \in \mathcal{N}^{\mathrm{c}}_{i,k} \cup \{i\}$ using the transform (24), (25), and the inverse (24).

The previous one-step ahead evaluation of $\mathcal{P}^{\mathrm{p}}_{i,m,k+1}$ is applied recursively to get $\mathcal{P}^{\mathrm{p}}_{i,k+h}$. UAV i can then search for $\mathbf{u}_{i,k:k+h-1}$ minimizing $\Phi^{\mathrm{B}}(\mathcal{P}^{\mathrm{p}}_{i,k+h}, \underline{p})$. When h is small, $\mathbf{u}_{i,k:k+h-1}$ may have no impact on $\Phi^{\mathrm{B}}(\mathcal{P}^{\mathrm{p}}_{i,k+h}, \underline{p})$. Consequently, the alternative cost function

$$J^{\mathrm{B}}\left(\mathbf{u}_{i,k:k+h-1}\right) = \Phi^{\mathrm{B}}(\mathcal{P}^{\mathrm{p}}_{i,k+h}, \underline{p}) + \alpha^{\mathrm{B}} d_{\mathrm{B}}(\mathbf{x}^{\mathrm{u,p}}_{i,k+h}, \mathcal{P}^{\mathrm{p}}_{i,k+h}), \tag{27}$$

is introduced, where

$$d_{\mathrm{B}}(\mathbf{x}^{\mathrm{u,p}}_{i,k+h}, \mathcal{P}^{\mathrm{p}}_{i,k+h}) = \min_{m \in \mathcal{N}^{\mathrm{c}}, 1-\underline{p}' < p^{m,\mathrm{p}}_{i,k+h} < \underline{p}'} ||\mathbf{c}_m - \mathbf{x}^{\mathrm{u,p}}_{i,k+h}||,$$

where $\mathbf{c}_m$ is the center $\mathcal{C}_m$. The distance $d_{\mathrm{B}}(\mathbf{x}^{\mathrm{u,p}}_{i,k+h}, \mathcal{P}^{\mathrm{p}}_{i,k+h})$ helps driving UAVs to cells for which the presence of targets is still uncertain (determined by the threshold $\underline{p}'$). The weight α^{B} balances the relative importance of this distance with respect to the first term of (27) and plays a role similar to the one of α^{SM}.

5. SIMULATIONS

Simulation conditions are provided in Section 5.1. The performance of the SM and stochastic estimators is first compared in a scenario without false positive detection in Section 5.2. Three different sources of false positive detection are then considered. Section 5.3 reports results where false positive detection is due to the presence of false targets, whose detection conditions are deterministic, as in Ibenthal et al. (2021). Then, Sections 5.4 and 5.5 report results where false positive detection is random to model a defective or imperfect sensor or changing environmental conditions.

5.1 Simulation conditions

In the following simulations, the sampling period is $T = 0.5\,\mathrm{s}$. The RoI is a square of $500 \times 500\,\mathrm{m}^2$. A fleet of $N^{\mathrm{u}} = 4$ UAVs searches for $N^{\mathrm{t}} = 10$ *static* ground targets uniformly distributed in the RoI. The state of UAV i at time t_k consists of its location $\boldsymbol{x}^{\mathrm{u}}_{i,k} = (x^{\mathrm{u}}_{i,k,1}, x^{\mathrm{u}}_{i,k,2}, x^{\mathrm{u}}_{i,k,3})^\top$, flight path angle $x^{\mathrm{u}}_{i,k,4}$, heading angle $x^{\mathrm{u}}_{i,k,5}$, yaw rate $x^{\mathrm{u}}_{i,k,6}$, and yaw rate derivative $x^{\mathrm{t}}_{i,k,7}$. The UAVs move at a constant altitude of $h = 100\,\mathrm{m}$ and a constant speed of $V = 16.6\,\mathrm{m/s}$. The control input $u_{i,k}$ is limited to the yaw rate $x^{\mathrm{u}}_{i,k,7}$. The state vector $\mathbf{x}^{\mathrm{u}}_{i,k}$ evolves according to

$$\begin{pmatrix} x^{\mathrm{u}}_{i,k+1,1} \\ x^{\mathrm{u}}_{i,k+1,2} \\ x^{\mathrm{u}}_{i,k+1,3} \\ x^{\mathrm{u}}_{i,k+1,4} \\ x^{\mathrm{u}}_{i,k+1,5} \\ x^{\mathrm{u}}_{i,k+1,6} \\ x^{\mathrm{u}}_{i,k+1,7} \end{pmatrix} = \begin{pmatrix} x^{\mathrm{u}}_{i,k,1} + T\cos\left(x^{\mathrm{u}}_{i,k,4}\right)\cos\left(x^{\mathrm{u}}_{i,k,5}\right)V \\ x^{\mathrm{u}}_{i,k,2} + T\cos\left(x^{\mathrm{u}}_{i,k,4}\right)\sin\left(x^{\mathrm{u}}_{i,k,5}\right)V \\ x^{\mathrm{u}}_{i,k,3} + T\sin\left(x^{\mathrm{u}}_{i,k,4}\right)V \\ x^{\mathrm{u}}_{i,k,4} \\ x^{\mathrm{u}}_{i,k,5} + T x^{\mathrm{u}}_{i,k,6} \\ x^{\mathrm{u}}_{i,k,6} + T x^{\mathrm{u}}_{i,k,7} \\ u_{i,k} \end{pmatrix}.$$

The FoVs are half cones with an identical aperture of $\pi/4$ for the azimuth and elevation. Their inclination with respect to the body X axis (roll axis) is $\gamma_{\mathrm{FoV}} = 3\pi/8$. When a target is detected, a noisy measurement of its state is obtained, with a noise uniformly distributed in $[-5, 5] \times [-5, 5]\,\mathrm{m}^2$. To reflect a partial knowledge of the noise bounds, which have to be over estimated, one takes $[\mathbf{w}] = [-7, 7] \times [-7, 7]\,\mathrm{m}^2$. The prediction horizon for the control design is $h = 3$ for both control schemes. The RoI is divided into 125×125 cells for the probability map of the Bayesian estimator. Each cell has a size of $4 \times 4\,\mathrm{m}$. The results have been averaged over 30 independent simulations with uniformly distributed initial locations of the targets and UAVs in the RoI.

In the SM approach, the value α^{SM} in (17) has to be chosen so that $\alpha^{\mathrm{SM}} d(\mathbf{x}^{\mathrm{u,p}}_{i,k+h}, \mathbb{X}^{\mathrm{p}}_{i,k+h} \cup \overline{\mathbb{X}}^{\mathrm{p}}_{i,k+h})$ remains small compared to $\Phi^{\mathrm{SM}}(\mathbb{X}^{\mathrm{p}}_{i,k+h}, \overline{\mathbb{X}}^{\mathrm{p}}_{i,k+h})$, to emphasize the reduction of the size of the sets. Sets are represented using Matlab polyshapes.

In the Bayesian approach, four parameters need to be chosen. The thresholds $\underline{p}$ and $\underline{p}'$ for $p^m_{i,k}$ determine when one decides a target is present or absent in a cell. The weight α^{B} has a similar meaning as α^{SM} and should be chosen such that $\alpha^{\mathrm{B}} d^{\mathrm{B}}(\boldsymbol{x}^{\mathrm{u,P}}_{i,k+h}, \mathcal{P}^{\mathrm{P}}_{i,k+h})$ remains small compared to $\Phi^{\mathrm{B}}(\mathcal{P}^{\mathrm{p}}_{i,k+h})$. Finally, the false detection probability q needs to be selected. This probability depends on the quality of observation and thus on the sensor, the image processing system, and environmental conditions. The value of q may be derived from prior simulations and experiments analyzing the properties of the sensor system in various conditions. Here, the parameters are chosen as $\alpha^{\mathrm{SM}} = \alpha^{\mathrm{B}} = 0.0001$ and $\underline{p}' = 0.99$.

5.2 Without false positive detection

In the first scenario, the estimation performance is compared without false positive detection. Figure 4 (left) presents the evolution of $\overline{\Phi}^{\mathrm{SM}}_k = \frac{1}{N^{\mathrm{u}}} \sum_{i=1}^{N^{\mathrm{u}}} \Phi^{\mathrm{SM}}(\mathbb{X}_{i,k}, \overline{\mathbb{X}}_{i,k})$ and $\overline{\Phi}^{\mathrm{B}}_k\left(\underline{p}\right) = \frac{1}{N^{\mathrm{u}}} \sum_{i=1}^{N^{\mathrm{u}}} \Phi^{\mathrm{B+}}\left(\mathcal{P}_{i,k}, \underline{p}\right)$, with $\Phi^{\mathrm{B+}}\left(\mathcal{P}_{i,k}, \underline{p}\right) =$

$\left|\{m \in \mathcal{N}^{\mathrm{c}} \mid p_{i,k}^{m} \geqslant \underline{p}\}\right| / N^{\mathrm{c}}$, $\underline{p} \in \{0.6, 0.9, 0.99\}$. As soon as $\overline{\mathbb{X}}_{i,k} = \emptyset$, $\overline{\Phi}_k^{\mathrm{SM}}$ and $\overline{\Phi}_k^{\mathrm{B}}(\underline{p})$ provide the proportion of the search area where the estimators conclude in the presence of targets. For the Bayesian approach, three values for the probabilities of false positive detection are compared $q \in \{0.1, 0.5, 0.9\}$. Some values are chosen very large to emphasize their impact on the estimation performance.

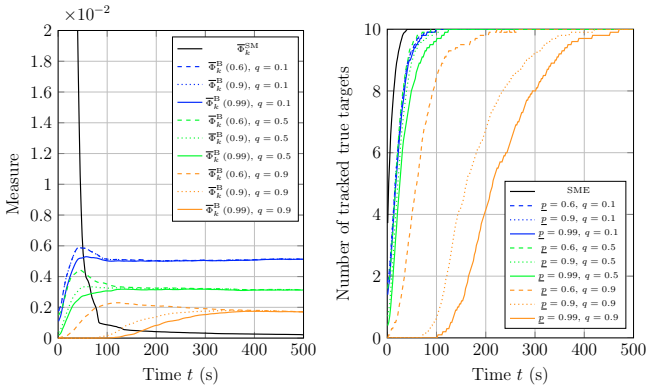

Fig. 3. Without false detection: Mean values of $\overline{\Phi}_k^{\mathrm{SM}}$ and $\overline{\Phi}_k^{\mathrm{B}}(\underline{p})$ (left) and of the number of true targets tracked (right).

Figure 3 (left) shows that $\overline{\Phi}_k^{\mathrm{SM}}$ monotonically decreases with t_k and converges to 0.064×10^{-2}, which is the number of true targets ($N^{\mathrm{t}} = 10$) times the measure of the mismatch of the noise bound ($(\pm 2) \times (\pm 2)\ \mathrm{m}^2$) divided by the area of the RoI ($500 \times 500\,\mathrm{m}^2$). The proposed SM estimator evaluates guaranteed estimates (provided that the assumptions on the noise bounds are satisfied). Consequently, $\overline{\Phi}_k^{\mathrm{SM}}$ is an upper bound for the estimation uncertainty that can be obtained.

For the Bayesian estimator, the criterion $\overline{\Phi}_k^{\mathrm{B}}(\underline{p})$ converges towards different values depending on $q \in \{0.1, 0.5, 0.9\}$. The smallest value of $\overline{\Phi}_k^{\mathrm{B}}(\underline{p})$ is identical to that of $\overline{\Phi}_k^{\mathrm{SM}}$ and corresponds to N^{t} times the area of a single cell ($4 \times 4\,\mathrm{m}^2$) divided by the area of the RoI. Nevertheless, due to the mismatch of the noise bound, a single target may lead to a constant detection in neighboring cells. Assuming that a single target leads to a detection of targets in 3 neighboring cells results in a final value of $\overline{\Phi}_k^{\mathrm{B}}(\underline{p})$ of 0.192×10^{-2}, which is very close to what is obtained for $\overline{\Phi}_k^{\mathrm{B}}(0.99)$, when $q = 0.9$. The Bayesian estimator with $q = 0.9$ performs better since it removes more efficiently these erroneous detections in neighboring cells.

Figure 3 (right) presents the number of tracked targets. For the SM estimator, it is number of targets that are located in $\mathbb{X}_{i,k}$ (solid, black, SME). The targets are always located in $\mathbb{X}_{i,k} \cup \overline{\mathbb{X}}_{i,k}$. For the Bayesian estimator, it is the number of targets in cells with $p_{i,k}^{m} > \underline{p}$. The Bayesian estimator with $q = 0.9$ needs a much larger number of observations to identify the cells where the targets are located. This is reasonable since the higher probability of false positive detection makes it necessary to collect more measurements of the same cell to increase $p_{i,k}^{m}$.

5.3 Deterministic false positive detection

In this section, static false targets may be confused with true targets. A false target at location $\mathbf{x}_j^{\mathrm{f}}$ is detected when $\mathbf{x}_j^{\mathrm{f}} \in \mathbb{F}_i(\mathbf{x}_{i,k}^{\mathrm{u}})$. When detected, the false target is confused with a true target when $\mathbf{x}_{i,k}^{\mathrm{u}} \notin g_j(\mathbf{x}_j^{\mathrm{f}})$, where

$g_j(\mathbf{x}_j^{\mathrm{f}}) = \{\mathbf{x}_j^{\mathrm{f}} + \sum_{m=1}^{3} a_m \boldsymbol{v}_{j,m} \mid a_m \in \mathbb{R}^+, m = 1, 2, 3\}$, is a half cone described by vectors $\boldsymbol{v}_{j,1}$, $\boldsymbol{v}_{j,2}$, and $\boldsymbol{v}_{j,3} \in \mathbb{R}^3$. One has $\boldsymbol{v}_{j,1} = (0, 0, 1)^{\top}$. The angle between vectors are $\angle(\boldsymbol{v}_{j,1}, \boldsymbol{v}_{j,2}) = \pi/4$, $\angle(\boldsymbol{v}_{j,1}, \boldsymbol{v}_{j,3}) = \pi/4$, and $\angle(\boldsymbol{v}_{j,2}, \boldsymbol{v}_{j,3}) = \pi/4$. The orientation/angle of the cone $\angle(\boldsymbol{v}_{j,2}, (1, 0, 0)^{\top})$ is uniformly distributed in $[0, 2\pi[$. When $\boldsymbol{x}_{i,k}^{\mathrm{u}} \in g_j(\mathbf{x}_j^{\mathrm{f}})$, the measurement is discarded, which translates the fact that the UAV observes the target with a point of view that enables determining that it is a false target, see also Ibenthal et al. (2021). Consequently, for $\mathcal{Y}_{i,k}$ in (3), if $\mathbf{x}_j^{\mathrm{f}} \in \mathbb{F}_i(\mathbf{x}_{i,k}^{\mathrm{u}})$ and $\boldsymbol{x}_{i,k}^{\mathrm{u}} \notin g_j(\mathbf{x}_j^{\mathrm{f}})$ then there exists $\mathbf{y} \in \mathcal{Y}_{i,k}$ such that $\mathbf{y} = \mathbf{y}_{i,j,k}^{\mathrm{f}}$ where $\mathbf{y}_{i,j,k}^{\mathrm{f}} = \mathbf{h}_i(\mathbf{x}_{i,k}^{\mathrm{u}}, \mathbf{x}_j^{\mathrm{f}}) + \mathbf{w}_{i,j,k}$ is the measurement of the location $\boldsymbol{x}_j^{\mathrm{f}}$ of false target j with $\mathbf{w}_{i,j,k}$ uniformly distributed in $[-5, 5] \times [-5, 5]\,\mathrm{m}^2$. The RoI contains 10 uniformly distributed false targets.

Figure 4 (left) shows that $\overline{\Phi}_k^{\mathrm{SM}}$ is not much affected by the presence of false targets, compared to Figure 3 (left). For the stochastic estimator, $\overline{\Phi}_k^{\mathrm{B}}(\underline{p})$ converges to different values compared to Figure 3. The estimator with $q = 0.1$ is strongly affected by the presence of the false targets and $\overline{\Phi}_k^{\mathrm{B}}(0.99)$ converges to 0.9×10^{-2} (compared to 0.5×10^{-2} in Figure 3).

Figure 4 (right) shows the evolution of the number of tracked true targets. The presence of 10 false targets does not impact significantly the SM estimator. The Bayesian estimator shows also a similar behavior. Nevertheless, the number of tracked targets for the estimator with $\underline{p} = 0.99$ and $q = 0.9$ is increasing faster around $t = 200$ s than in Figure 3 (right). Repetitive observations of false targets seem to lead also to more observations of true targets and thus to improved detection of the true targets.

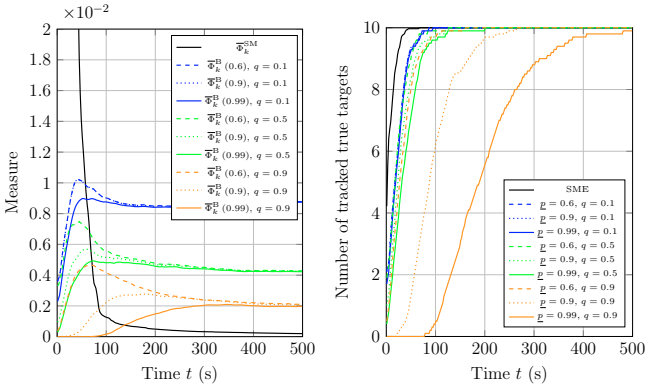

Fig. 4. Deterministic false positive detection: Mean values of $\overline{\Phi}_k^{\mathrm{SM}}$ and $\overline{\Phi}_k^{\mathrm{B}}(\underline{p})$ (left) and of the number of true targets tracked (right).

Figure 5 shows the mean values of the number of tracked false targets, *i.e.*, false targets that are inside the set

estimates $\mathbb{X}^{\mathrm{U}}_{i,k} \cup \overline{\mathbb{X}}_{i,k}$ (for the SM estimator) or inside a cell m, where $p^m_{i,k} > \underline{p}$ (for the stochastic estimator). One observes that the stochastic estimator with $q = 0.9$ is the most efficient in discarding locations of false targets, and performs the worst with $q = 0.1$. A high probability of false positive detection forces the UAVs to update the probability of each cell many times to reach $p^m_{i,k} > \underline{p}'$ as in (27), since the presence or absence of a target is considered uncertain if $1 - \underline{p}' < p^m_{i,k} < \underline{p}'$. The frequent updates lead to changing points of view when collecting observations, and the UAVs are prone to attain configurations where $\boldsymbol{x}^{\mathrm{u}}_{i,k} \in g_j\left(\mathbf{x}^{\mathrm{f}}_j\right)$ and can finally discard the false targets.

The stochastic estimator with $q \leqslant 0.5$ performs worse than the SM estimator in eliminating false targets. This might be partially due to numerical approximations. The probability $p^m_{i,k}$ in each cell may be rounded to either 0 or 1 after a finite number of observations, which leads to $q^m_{i,k}$ either $+\infty$ or $-\infty$. As a consequence, the cost function (27) can become zero whatever the control input sequence.

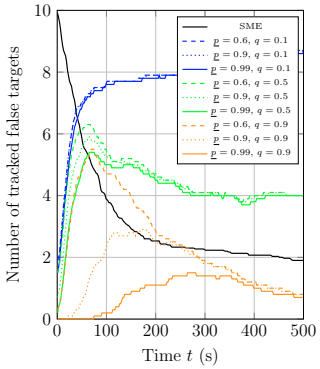

Fig. 5. Deterministic false positive detection: Mean values of the number of tracked false targets.

5.4 Stochastic false positive detection: Poisson model

In this section, false positive detection are assumed to be due to a defective/imperfect sensor or computer vision system. At each time t_k UAV i may get $N^{\mathrm{f}}_{i,k}$ false positive detection in the FoV, where $N^{\mathrm{f}}_{i,k}$ follows a Poisson distribution with parameter λ_i, determined by the quality of the computer vision system of UAV i, *i.e.*, $P(N^{\mathrm{f}}_{i,k} = n \mid \lambda_i) = \lambda_i^n \mathrm{e}^{-\lambda_i}/n!$. The locations of the $N^{\mathrm{f}}_{i,k}$ false detection is uniformly distributed in $\mathbb{F}_i(\mathbf{x}^{\mathrm{u}}_{i,k})$. Each false positive detection generates a measurement $\mathbf{y}$ in $\mathcal{Y}_{i,k}$.

Figure 6 presents the performance of the estimators when $\lambda_i = 10$. The evolution of the number of tracked targets of the SM estimator in Figure 6 (right) is very similar to that in absence of false detection. The Bayesian estimator with $q = 0.9$ converges towards similar values $\overline{\Phi}^{\mathrm{B}}_k(0.99) \approx 0.2 \times 10^{-2}$. One observes that targets are detected earlier for a higher probability of false positive detection. This false positive detection model has a strong impact on the performance of the Bayesian estimator with $q = 0.1$. One observes a strong overshoot of $\overline{\Phi}^{\mathrm{B}}_k(0.99)$ with $q = 0.1$ and $\lambda_i = 10$ and a convergence to $\overline{\Phi}^{\mathrm{B}}_k(0.99) \approx 0.8 \times 10^{-2}$. This indicates that the chosen probability of false positive detection ($q = 0.1$) is too small and the real probability of false positive detection is higher. In general, an appropriate choice of q should lead to an evolution of $\Phi^{\mathrm{B}}\left(\mathcal{P}_{i,k}, \underline{p}\right)$ that does not present any overshoots.

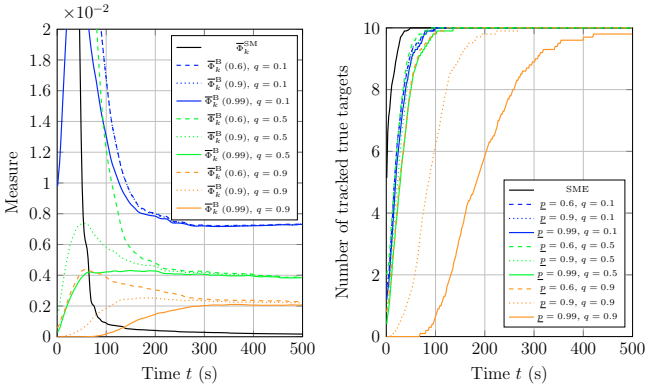

Fig. 6. Stochastic false positive detection – Poisson model with $\lambda_i = 10$: Mean values of $\overline{\Phi}^{\mathrm{SM}}_k$ and $\overline{\Phi}^{\mathrm{B}}_k\left(\underline{p}\right)$ (left) and of the number of tracked true targets (right).

5.5 Stochastic false positive detection: Markov model

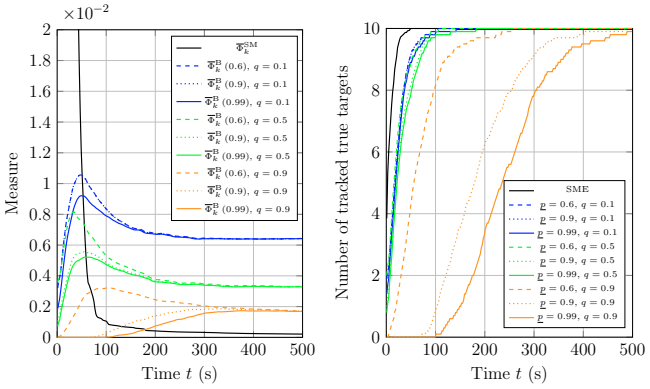

Fig. 7. Stochastic false positive detection – Markov model: Results of simulations with $p_{11} = 0.99$ and $p_{00} = 1 - 7.10^{-6}$. Mean values of $\overline{\Phi}^{\mathrm{SM}}_k$ and $\overline{\Phi}^{\mathrm{B}}_k\left(\underline{p}\right)$ (left) and of the number of true targets tracked (right).

Now, false positive detection is assumed to be due to changing environmental conditions. The false positive detection in $\mathcal{C}_m$, $m \in \mathcal{N}^{\mathrm{c}}$, is modeled by a Markov process. At time t_k, consider N^{c} independent and identically distributed stationary binary Markov processes $\theta^{m,\mathrm{f}}_k$ to model potential false positive detection of a target in $\mathcal{C}_m$. When $\theta^{m,\mathrm{f}}_k = 1$, a target is erroneously detected in cell $\mathcal{C}_m$ when observed. When $\theta^{m,\mathrm{f}}_k = 0$, no false positive detection occurs when $\mathcal{C}_m$ is observed. The UAVs have no access to $\theta^{m,\mathrm{f}}_k$. The evolution of $\theta^{m,\mathrm{f}}_k$ represents changes in environmental conditions. The state transition probabilities are $\Pr(\theta^{m,\mathrm{f}}_{k+1} = 1 \mid \theta^{m,\mathrm{f}}_k = 1) = p_{11}$ and $\Pr(\theta^{m,\mathrm{f}}_{k+1} = 0 \mid \theta^{m,\mathrm{f}}_k = 0) = p_{00}$. If at time t_k, $\theta^{m,\mathrm{f}}_k = 1$ and $\mathcal{C}_m \subset \mathbb{F}_i(\mathbf{x}^{\mathrm{u}}_{i,k+1})$ UAV i gets an additional measurement $\mathbf{y}$ that corresponds to the detection of a decoy at the center of $\mathcal{C}_m$.

Figure 7 presents the estimation performance of the two estimators with $p_{11} = 0.99$ and $p_{00} = 1 - 7.10^{-6}$. This choice produces in average 10 cells in the RoI where $\theta_k^{m,\mathrm{f}} = 1$. At $k = 0$, 10 randomly selected cells are such that $\theta_0^{m,\mathrm{f}} = 1$. The others are initialized with $\theta_k^{m,\mathrm{f}} = 0$. Again, the SM estimator is hardly affected by the presence of false positive detection, contrary to the Bayesian estimation, which convergence speed is reduced.

6. CONCLUSION AND PERSPECTIVES

This paper compares SM and stochastic Bayesian state estimators for target search and tracking. Both estimation techniques are applied to search scenarios with false targets and a potentially defective/imperfect computer vision system. It is assumed that the detection of false targets is deterministic and depends on the points of view of the UAVs when an observation is taken. Stochastic false positive detection is assumed to be caused by a defective/imperfect computer vision system, where the false positive detection appears uniformly distributed in the FoV. The results show that the SM estimator is quite insensitive to the considered sources of false positive detection. The stochastic estimator presents a higher sensitivity.

Furthermore, the choice of the assumed probability of false positive detection q impacts the estimation uncertainty considerably. Consequently, q is an additional parameter that must be carefully chosen when using a stochastic estimation method. The stochastic estimator shows the potential to remove false targets more effectively from the estimates when choosing a very high probability of false positive detection. Nevertheless, this also delays the estimation of the location of true targets.

Further extensions of the comparison include simulation with moving targets and other noise sources. Only false positive detection is considered in this paper. It would be very interesting to adapt and compare both estimation techniques for scenarios where false negative detection of targets may appear. The adaptation of the stochastic estimator in this context seems to be simpler than for the SM estimator.

REFERENCES

Bertuccelli, L.F. and How, J. (2005). Robust UAV search for environments with imprecise probability maps. In *Proc. IEEE CDC*, 5680–5685.

Bertuccelli, L.F. and How, J.P. (2006a). Search for dynamic targets with uncertain probability maps. In *Proc. American Contr. Conf.*, 6–pp.

Bertuccelli, L.F. and How, J.P. (2006b). UAV search for dynamic targets with uncertain motion models. In *Proc. IEEE CDC*, 5941–5946.

Boukezzoula, R., Jaulin, L., Desrochers, B., and Foulloy, L. (2021). Thick gradual sets and their computations: Application for determining the uncertain zone explored by an underwater robot. *Eng. Appl. Artif. Intel.*, 102, 104287.

Cortes, J., Martinez, S., Karatas, T., and Bullo, F. (2004). Coverage control for mobile sensing networks. *IEEE Trans. Robotics and Autom.*, 20(2), 243–255.

Desrochers, B. and Jaulin, L. (2016). Computing a guaranteed approximation of the zone explored by a robot. *IEEE Trans. Aut. Contr.*, 62(1), 425–430.

Drevelle, V., Jaulin, L., and Zerr, B. (2013). Guaranteed characterization of the explored space of a mobile robot by using subpavings. *IFAC Proc. Vol.*, 46(23), 44–49.

Frew, E.W. and Elston, J. (2008). Target assignment for integrated search and tracking by active robot networks. In *Proc. IEEE ICRA*, 2354–2359. Pasadena, USA.

Furukawa, T., Bourgault, F., Lavis, B., and Durrant-Whyte, H.F. (2006). Recursive Bayesian search-and-tracking using coordinated uavs for lost targets. In *Proc. IEEE ICRA*, 2521–2526.

Gu, F., He, Y., and Han, J. (2015). Active persistent localization of a three-dimensional moving target under set-membership uncertainty description through cooperation of multiple mobile robots. *IEEE Trans. Ind. Electron.*, 62(8), 4958–4971.

Hespanha, J.P., Kim, H.J., and Sastry, S. (1999). Multiple-agent probabilistic pursuit-evasion games. In *Proc. IEEE CDC*, volume 3, 2432–2437.

Hu, J., Xie, L., Lum, K.Y., and Xu, J. (2012). Multiagent information fusion and cooperative control in target search. *IEEE Trans. Cont. Syst. Tech.*, 21(4), 1223–1235.

Hu, J., Xie, L., Xu, J., and Xu, Z. (2014). Multi-agent cooperative target search. *Sensors*, 14(6), 9408–9428.

Hu, X., Liu, Y., and Wang, G. (2017). Optimal search for moving targets with sensing capabilities using multiple UAVs. *Jnl Syst. Eng. and Elect.*, 28(3), 526–535.

Ibenthal, J., Kieffer, M., Meyer, L., Piet-Lahanier, H., and Reynaud, S. (2021). Bounded-error target localization and tracking using a fleet of UAVs. *Automatica*, 132, 109809.

Ibenthal, J., Meyer, L., Kieffer, M., and Piet-Lahanier, H. (2020). Bounded-error target localization and tracking in presence of decoys using a fleet of UAVs. In *Proc. IFAC-PapersOnLine*, volume 53, 9521–9528.

Khan, A., Yanmaz, E., and Rinner, B. (2015). Information exchange and decision making in micro aerial vehicle networks for cooperative search. *IEEE Trans. Control Netw. Syst.*, 2(4), 335–347.

Kuhlman, M.J., Otte, M., Sofge, D., and Gupta, S.K. (2017). Multipass target search in natural environments. *Sensors*, 17(11), 2514.

Li, P. and Duan, H. (2017). A potential game approach to multiple UAV cooperative search and surveillance. *Aerosp. Sci. Technol.*, 68, 403–415.

Robin, C. and Lacroix, S. (2016). Multi-robot target detection and tracking: Taxonomy and survey. *Auton. Robot.*, 40(4), 729–760.

Vidal, R., Rashid, S., Sharp, C., Shakernia, O., Kim, J., and Sastry, S. (2001). Pursuit-evasion games with unmanned ground and aerial vehicles. In *Proc. IEEE ICRA*, volume 3, 2948–2955.

Yang, Y., Polycarpou, M.M., and Minai, A.A. (2007). Multi-UAV cooperative search using an opportunistic learning method. *J. Dyn. Sys., Meas., Control.*, 716–728.

Zhen, Z., Chen, Y., Wen, L., and Han, B. (2020). An intelligent cooperative mission planning scheme of UAV swarm in uncertain dynamic environment. *Aerospace Science and Technology*, 100, 105826.